Laser Cladding of Stellite-6 on AISI 316 L Austenitic Stainless Steel: Empirical-Statistical Modeling and Parameter Optimization

Jeferson Trevizan Pacheco [1,2] · Leandro João da Silva [3] ·
Luiz Delagnelo Barbetta [1] · Henrique Santos Ferreira [1] ·
Marcelo Taveira Veiga [1,2] · Renato Forni [4] · Moisés Felipe Teixeira [1,2,3,5]

Abstract

This work aimed to develop an empirical statistical model to determine the optimized parameters for depositing multi-bead single layer Stellite-6 coating on AISI 316 L austenitic stainless steel by laser cladding. A full factorial experimental design was carried out to establish a correlation between processing parameters (laser power, scanning speed and powder feed rate) and geometric characteristics of the coatings (dilution, peak height and surface waviness) through multiple regression. Optimized deposition parameters were estimated by desirability function and experimentally validated. The microstructure and microhardness were assessed as a mean of estimate the performance of optimized coating. The empirical-statistical model and optimization method proposed in this work were demonstrated to be valuable tools for process optimization with low computational cost. This would contribute for a higher material efficiency and reducing post-processing operations, such as machining. As expected for Stellite-6 coatings, the microstructure was composed of dendrites rich in cobalt and interdendritic regions composed of chromium carbides. The microhardness level corroborates the literature, suggesting that the performance was not compromised in favor of the coating geometry.

Keywords Laser cladding · Stellite-6 · Deposition parameters · Optimization

Introduction

Laser cladding is a hardfacing process that uses a high-power laser beam to melt the metal powder and a thin layer of substrate to form coating. Among several processing parameters of laser cladding process, those with the most significant impact on the

---

✉ Jeferson Trevizan Pacheco
  jeferson.tp@hotmail.com

Extended author information available on the last page of the article

coating characteristics are laser power [W], scanning speed [mm/min] and powder feed rate [g/min]. The deposition parameter selection for laser cladding is a difficult task and normally involve trial and error experiments [1]. Although there are precise computation simulations, these approaches yet demand high computational costs and highly qualified labor. In the absence of these resources, empirical-statistical modeling and numerical optimization approaches could be an alternative tool [2].

The use of statistical methods to estimate the deposition parameters for the laser cladding process is common in the current literature. However, these models are valid only for the tested conditions, e.g., laser type, optics, powder characteristics, substrate surface and processing window. Despite this, similar trends are expected. Nabhani et al. [1] studied the laser cladding of Ti-6Al-4 V. This study confirms the greater dependence of laser power, scanning speed and powder feed rate on the geometrical characteristics of the coatings. Davim et al. [3] investigated the laser cladding of Diamalloy (similar to type 420 stainless steel) and used multiple regression analysis to predict height, width and penetration of the coating. Farahmand et al. [4] used the Response Surface Methodology (RSM) with Central Composite Design (CCD) in order to optimize laser cladding of AISI H13. Lian et al. [5] used the RSM to evaluate the influence of laser power, scanning speed, and hatch distance (distance between beads) on the geometric characteristics of laser cladding of a medium carbon steel. The authors highlighted the importance to assess multiple parallel beads (coating an area) rather than single beads, which is usually reported in the literature.

In this scenario, the present work aimed to develop an empirical statistical model to determine the optimized parameters for deposition multi-bead single layer Stellite-6 coating on AISI 316 L austenitic stainless steel by laser cladding. A full factorial experimental design was carried out to establish a correlation between deposition parameters (laser power, scanning speed and powder feed rate) and geometric characteristics of the coatings (dilution, peak height and surface waviness) through multiple regression. Optimized deposition parameters were estimated by desirability function and experimentally validated. The microstructure and microhardness were assessed as a mean of estimate the performance of optimized coating. The main contributions of the present work were to present a parameter selection procedure to deposit coatings with desirable geometric characteristics by laser cladding, as well as, to confirm trend presented in the current literature.

Materials and Methods

Stellite-6 gas atomized powder was deposited by laser cladding on a substrate of AISI 316 L steel with dimensions of $15 \times 63 \times 250$ mm. The nominal chemical composition of the AISI 316 L substrate and the Stellite-6 powder are shown in Table 1 and Table 2, respectively.

Table 1 Nominal chemical composition of the substrate AISI 316 L steel

Element	Fe	Ni	Cr	Mo	Si	Mn	C	P
Composition [%]	Bal	10.88	16.38	2.30	0.50	1.22	0.02	0.03

Table 2 Nominal chemical composition of powder Stellite-6

Element	Co	Cr	W	Si	Fe
Composition [%]	Bal	27.83	2.48	0.65	0.06

The powder size distribution was measured by image dynamic analysis using a commercial equipment (Particle Insight®, Analyze Systems), and the result is shown in Table 3. As shown in Fig. 1.a, the powder particles tends to be spherical and present satellite particles (typical for gas atomized powders). The particles cross section analysis showed low porosity and dendritic microstructure as consequence of its rapid solidification, as shown in Fig. 1.b.

The laser cladding equipment used in this work is presented in Fig. 2. This system is equipped with a diode laser, with maximum power of 6000 W and wavelength of 1020 nm (Laserline model LDF6000-60VGP). The beam diameter on the plate surface and the stand-off distance were 5 mm and 15 mm, respectively. The laser source and powder feeder are connected to a coaxial deposition head (Fraunhofer Coax 8). Argon was used as shielding and carrier gas, with a flow rate of 15 l/min each.

Optimized coating microstructure was characterized through an optical microscope and Scanning Electron Microscopy (SEM). After standard metallographic preparation of the coatings cross sections (grinding and polishing), it was chemically attacked by immersion in regal water, with a concentration of 3:1 of HCl for HNO_3, for approximately 50 s to reveal the microstructure. Moreover, microhardness (HV 0.5) profiles were performed on the cross section of the coating.

Experimental Approach

The experimental approach of the present work is summarized in Fig. 3. The main deposition parameters are presented in Table 4, while the others were kept constant. The parameters used in the experiments were selected based on previous experiments, as well as, from current literature.

The coatings were obtained by depositing areas composed of 10 overlapped beads with length of 60 mm. As a general rule, the coatings were randomly deposited to mitigate systematic errors and the substrates alternated between depositions to keep a similar interpass temperature for all depositions.

Statistical Modeling

The open source R-Statistic software was used to develop the statistical modeling. The selected dependent variables (responses) were dilution, peak height and waviness. The

Table 3 Measured particle size distribution of metallic powder (equivalent diameter)

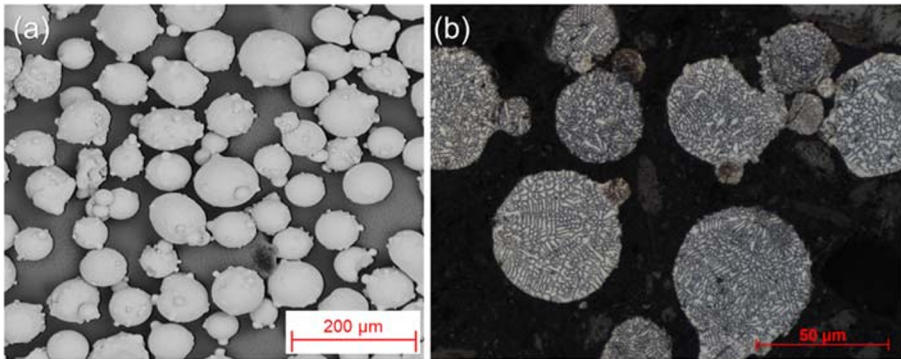| Dv 10% [μm]	Dv 50% [μm]	Dv 90% [μm]	Ø average [μm]
60.3	82.8	114.6	68.8

Fig. 1 (a) Particle morphology (Scanning Electron Microscopy - SEM) and (b) Transversal section analysis (Optical Microscope)

dilution was assessed by area method, defined by Eq. 1. Dilution is one of most important characteristics of the laser cladding coatings. On the one hand, low dilutions could generate lack of fusion [6] and, on the other hand, high dilution could be detrimental for coating performance [7, 8].

$$Dilution \ [\%] = \frac{A_{melted \ substrate \ area}}{A_{melted \ substrate \ area} + A_{deposited \ area}} *100\% \tag{1}$$

Peak height was considered as being the average between the peaks of each bead. The valley height was calculated similarly and the difference between both was defined as the coating surface waviness, defined by Eq. 2. A small height difference between peak and valley (surface waviness) is desirable to avoid excessive machining to obtain a flat surface. The geometric characteristics of the coating are shown in Fig. 4.

$$Waviness \ [mm] = Peak \ height - Valley \ height \tag{2}$$

The independent (depositions parameters) and dependent variables (geometric characteristics) of the model were correlated by multiple regressions, according to Eq. 3,

$$Y_i = \beta_n X_1^j X_2^k X_3^l \quad for \quad 2 \leq n \leq 64 \quad and \quad 0 \leq j, k, l \leq 3 \tag{3}$$
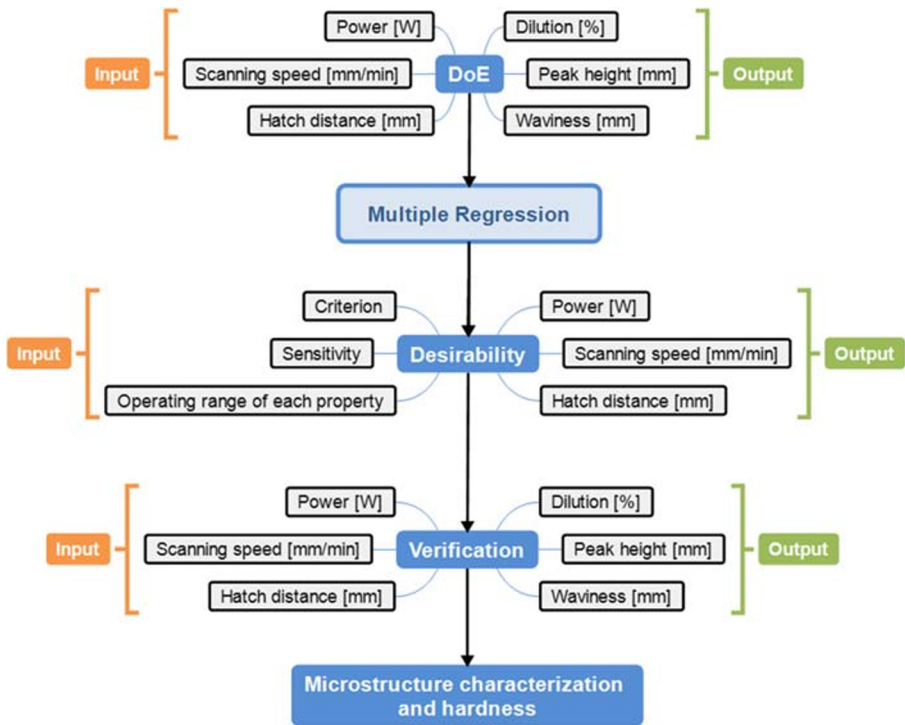

Fig. 2 Machine used in the experiment (Preco SL8600)

Fig. 3 Experimental approach workflow

where Y_i is the response (output), X_1 (P - Power), X_2 (V - Scanning speed) and X_3 (H - Hatch distance) are the input variables or parameters and β_n are the coefficients of the regression model, obtained through the minimum Mean Square Error (MSE) [9], given by Equation 4, where Y_i' are the approximate regression values for each input variable and N is the number of values analyzed. The response Y_i is provided 64 terms.

$$MSE = \frac{\sum_{i=1}^{N}\left(Y_i - Y_i'\right)^2}{N} \tag{4}$$

Although the multiple regression provides a good approximation for each response separately, it is necessary to seek the optimized processing condition by pondering all the responses of interest simultaneously. For that purpose, the desirability function

Table 4 Deposition parameters (independent variables)

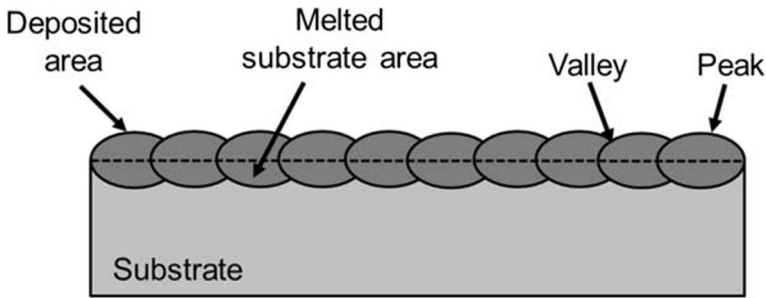|	
Laser power [W]	2600–3400 – 4200
Scanning speed [mm/min]	1200–1600 – 2000
Hatch distance [mm]	2.7–3.1 – 3.6
Powder feed rate [g/min]	40
Number of runs	27

Fig. 4 Geometric characteristics of the coating

methodology can be used [10]. Through this methodology, it is possible to consider all responses in a single function, given by Equation 5, where D is the overall desirability, m is the quantity of responses evaluated and d_i is the individual desirability of each response Y_i, in which it is evaluated with values between 0 and 1, where 0 can be defined as an unacceptable condition and 1 for the most desired condition.

$$D = \sqrt[m]{d_1 d_2 d_3 ... d_m} \tag{5}$$

The transformation of Y_i responses into d_i can be done in three different modes: optimal desirable (target value) (Equation 6), maximizing the response (Equation 7) or minimizing the response (Equation 8) [11]. The parameters s and t represent the sensitivity coefficients for the lower (I_i) and upper (S_i) limits for each variable, respectively, in a way that the higher the values of these parameters, the more restricted the tolerance will be, while T_i is the target value. The limits were established based on the literature and experiments previously carried out, and sensitivity coefficients were adjusted according to the desired response [2, 12, 13].

$$d_i(Y_i) = \begin{cases} 0 & if \quad Y_i < I_i \\ \left(\dfrac{Y_i - I_i}{T_i - I_i}\right)^s & if \quad I_i \leq Y_i \leq T_i \\ \left(\dfrac{Y_i - S_i}{T_i - S_i}\right)^t & if \quad T_i \leq Y_i \leq S_i \\ 0 & if \quad Y_i > S_i \end{cases} \tag{6}$$

$$d_i(Y_i) = \begin{cases} 0 & if \quad Y_i < I_i \\ \left(\dfrac{Y_i - I_i}{T_i - I_i}\right)^s & if \quad I_i \leq Y_i \leq T_i \\ 1 & if \quad Y_i > T_i \end{cases} \tag{7}$$

$$d_i(Y_i) = \begin{cases} 1 & if \quad Y_i < T_i \\ \left(\dfrac{Y_i - S_i}{T_i - S_i}\right)^s & if \quad T_i \leq Y_i \leq S_i \\ 0 & if \quad Y_i > S_i \end{cases} \tag{8}$$

Results

Cross sections and geometric parameters of all deposited coatings are summarized in Fig. 5. All tested conditions resulted in bead formation. An interesting characteristic observed was the increasing of the dilution during multiple beads depositions (covering an area), which could be linked with the accumulation of energy caused by sequential depositions [14].

Fig. 5 Cross sections and geometric parameters of obtained coatings (D = dilution [%], W = waviness [mm] and Ph = Peak height [mm])
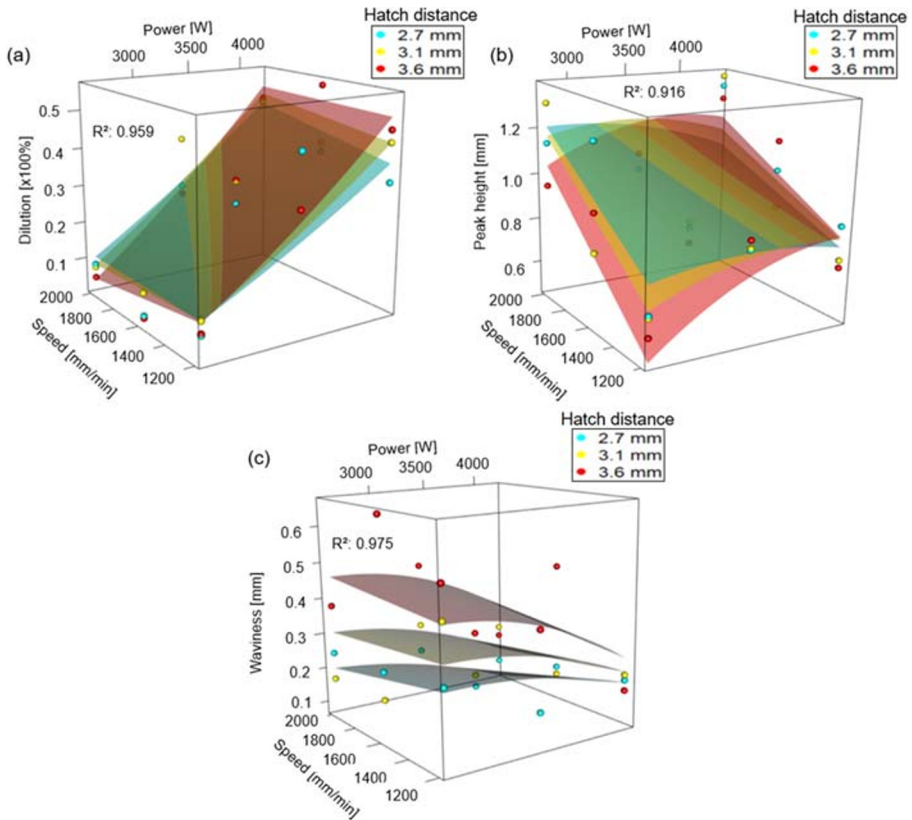
Fig. 6 Response surface for (a) dilution, (b) peak height and (c) waviness

The correlation equations for dilution [%], peak height [mm] and coating surface waviness [mm] as a function of laser power [W], scanning speed [mm/min] and powder feed rate [g/min] through multiple regression were:

$$Dilution\ [\%] = 2.18E^{-18}*P^2*H^2 - 5.94E^{-5}*V*H \atop + 4.58E^{-8}*P*V*H - 8.61E^{-9}*P*V*H^2 \tag{9}$$

$$Peak\ height\ [mm] = 2.76E^{-4}*P*H - 1.00E^{-8}*P^2*H^2 \atop -4.72E^{-8}*P*V*H \tag{10}$$

$$Waviness\ [mm] = 8.93E^{-5}*P*H - 5.07E^{-9}*P^2*H^2 - \atop 6.17E^{-8}*P*V*H + 1.81E^{-8}*P*V*H^2 \tag{11}$$

where P is power [W], V is scanning speed [mm/min] and H is hatch distance [mm].

The response surface of the coatings geometric characteristics for each hatch distance as a function of deposition parameters are shown in Fig. 6. The desirability
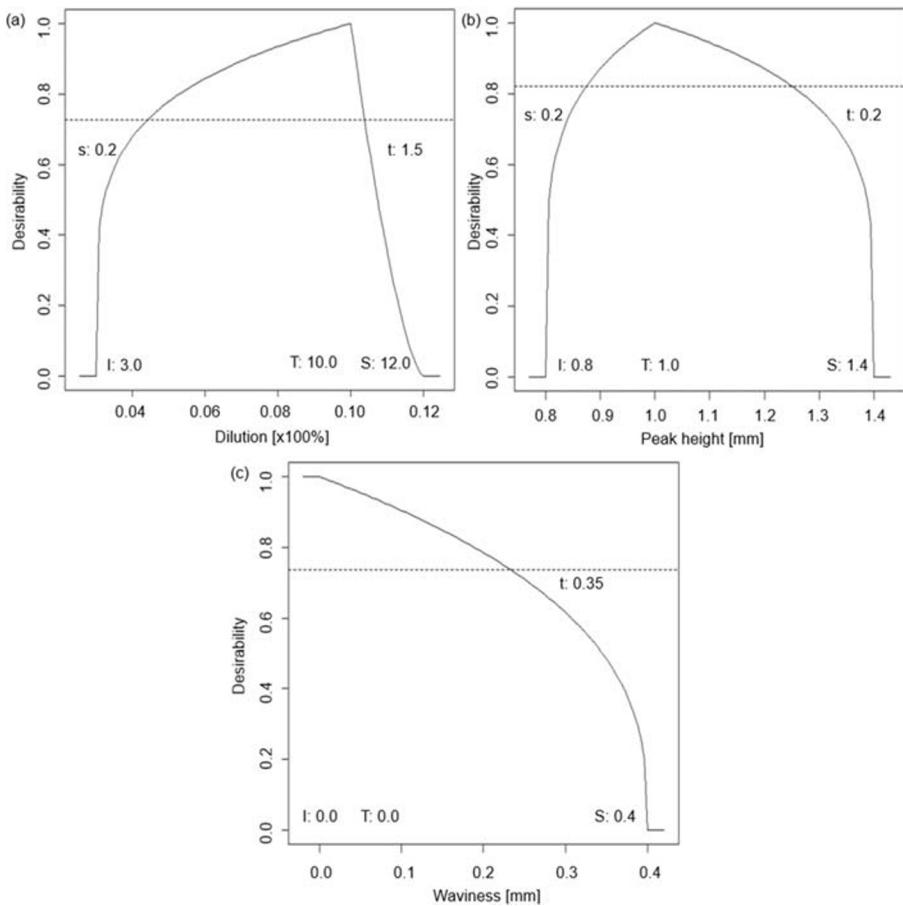
Fig. 7 Desirability curves for (a) dilution, (b) peak height and (c) waviness

optimization conditions for dilution, peak height and surface waviness are summarized in Fig. 7. The values of the estimated parameters given by the desirability function are shown in Table 5. The total desirability found was 0.8861.

Discussions

The response surface for the dilution is represented in Fig. 6.a. As expected, the laser power had a greater influence on dilution than scanning speed. This behavior can be explained considering that as the higher the laser power, the higher volume melted in

Table 5 Estimated optimized parameters by desirability function

Power [W]	3100
Speed [mm/min]	1420
Hatch distance [mm]	2.7

Fig. 8 Cross section of the coating obtained on the validation test

the substrate due to higher energy density (ED) [15]. The ED [J/mm^2] is given by Equation 12, where P is power [W], δ is laser beam diameter [mm] and V is scanning speed [mm/min] [16]. The dilution could be decreased by increasing the scanning speed [17, 18]. Moreover, the dilution level tends be higher as the higher the hatch distance, which can be related with a higher interaction between laser beam and substrate surface.

$$ED = \frac{P}{\delta V} \tag{12}$$

Figure 6. b shows the response surface for the peak height of the coatings. It can be observed that the scanning speed had greater impact on the peak heigh than the laser power. As the higher the scanning speed, the lower the peak height due to the lower the deposition rate by length unit. The coating peak height tends to be higher as lower the hatch distance, which could be related with a higher overlapping between the beads.

As observed in Fig. 6.c, both the laser power and the scanning speed had small impact on the response surface for the coating surface waviness. However, as the higher the hatch distance the higher the surface waviness. This observation heighted the importance of to assess the deposition parameter covering an area (multiple beads) rather than analyses performed on single beads.

Validation of Optimized Parameters

The coating deposited using the optimized parameters estimated by desirability function presented sound visual aspect and to be free of superficial defects. From cross section analysis presented in Fig. 8, can be seen that there is internal defects, such as lack of fusion and cracks.

Table 6 presents a comparison between the geometric characteristics of the estimated and experimental coating. It was observed that all experimentally obtained values are within the desirability function limits showed in Fig. 7.

Table 6 Comparison between experimental and estimated values

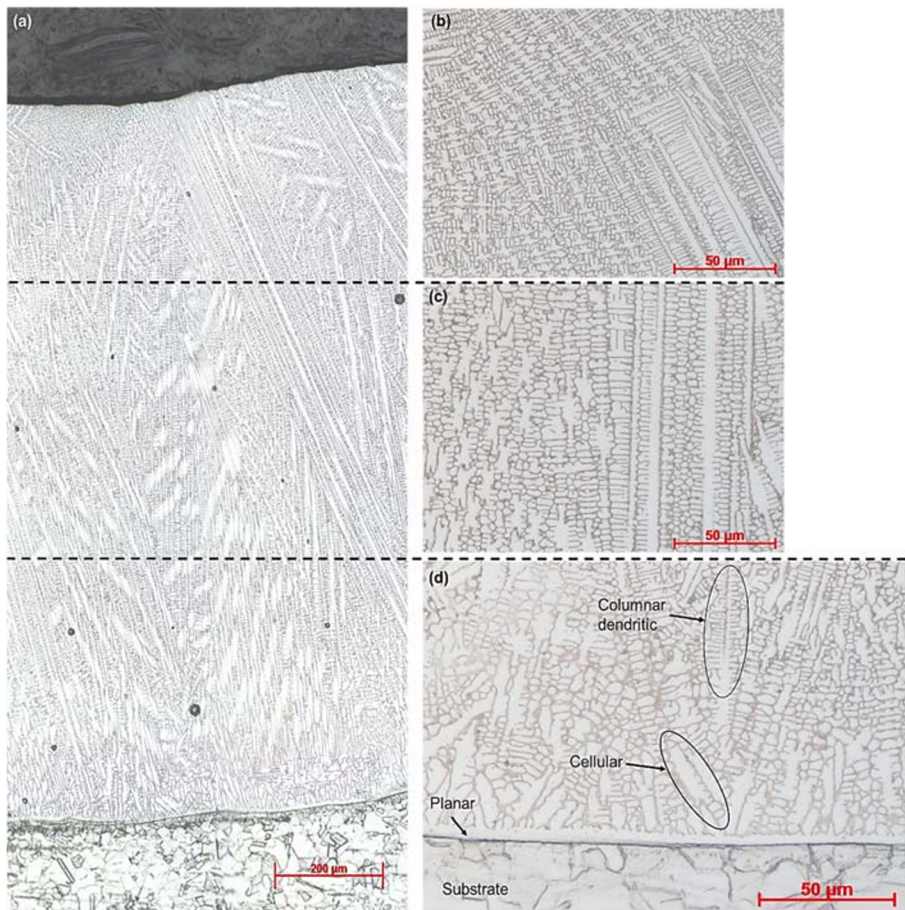| Geometric characteristics	Experimental	Estimated	Error [%]
Dilution [%]	12.10	11.10	9.00
Peak height [mm]	1.14	1.15	0.87
Waviness [mm]	0.16	0.15	6.67

Fig. 9 Solidification structure along the cross section of the coating: (a) coating cross section, (b) top, (c) middle and (d) interface between coating and substrate

The microstructure of the optimized coating is presented in Fig. 9. As expected, the solidification structure varied from planar to cellular and columnar dendritic. The finer solidification microstructure observed is a consequence of the high cooling rate imposed by laser cladding [19].

A more detailed characterization of the coating microstructure is presented in Fig. 10. It can be noted that the microstructure of the coating is composed of dendrites rich in cobalt, and the interdendritic region consists mainly of chromium carbides, corroborating the literature [20].

The microhardness of the coating was measured through the cross section, from the top of the coating towards the substrate. It was observed that the microhardness of the coating obtained average values around 500 HV, remaining homogeneous throughout the layer, as shown in Fig. 11. According to the literature available for this alloy and similar processing conditions, the values found are consistent [19, 21]. Moreover, these results suggesting that the performance was not compromised in favor of the coating geometry.
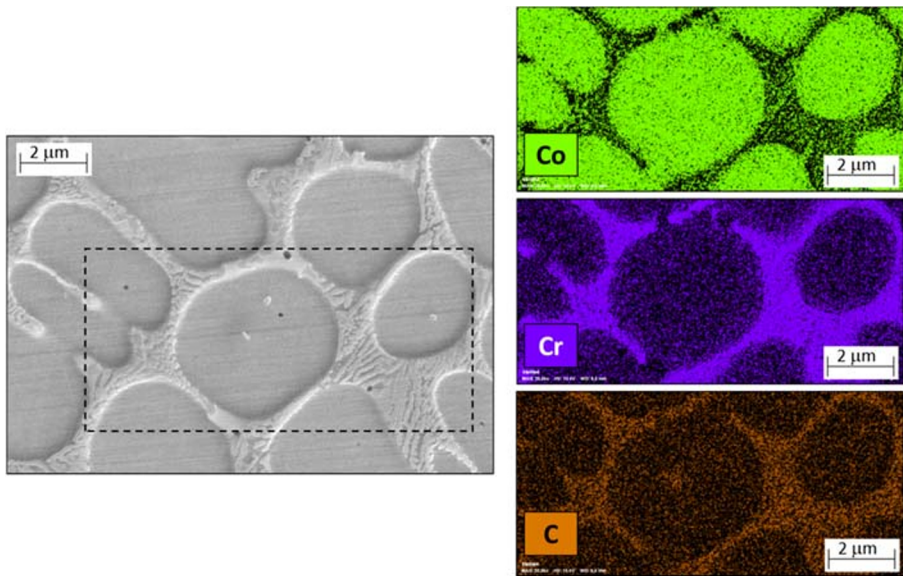
Fig. 10 SEM analysis: microstructure and elemental maps

Conclusions

The present work aimed to develop an empirical statistical model to determine optimized parameters for deposition multi-bead single layer Stellite-6 coating on AISI
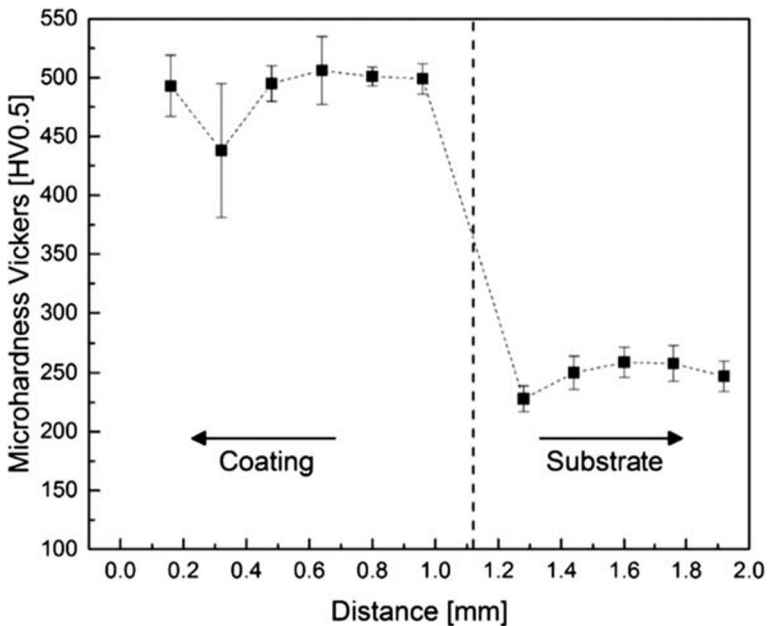

Fig. 11 Microhardness profile at coating cross section

316 L austenitic stainless steel by laser cladding. Based on the presented results, the following conclusions can be drawn:

– The empirical-statistical modeling and optimization showed as being a valuable tool with low computational cost to estimated deposition parameters to obtain coatings with desirable geometric characteristics.
– The geometric characteristics of the coating obtained in the validation experiment reached the limits imposed on the desirability function, showing small differences in relation to the values estimated by the empirical-statistical model.
– The dilution showed greater dependence of laser power followed by to scanning speed. For the surface peak height, it was noted that lower scanning speeds provide higher beads. For the waviness, there was dependence on hatch distance values.
– The microstructure of the coating is composed of dendrites rich in cobalt, and the interdendritic region consists mainly of chromium carbides.
– The microhardness of the coating showed homogeneity throughout the coating its cross section.

It is worth mentioning that the proposed model is valid for the tested conditions (laser cladding system and alloy). However, similar trends are expected for others experimental rigs and alloys.

References

1. Nabhani, M., Razavi, R.S., Barekat, M.: An empirical-statistical model for laser cladding of Ti-6Al-4V powder on Ti-6Al-4V substrate. Opt Laser Technol. **100**, 265–271 (2018). https://doi.org/10.1016/j.optlastec.2017.10.015
2. de Oliveira, U., Ocelík, V., De Hosson, J.T.M.: Analysis of coaxial laser cladding processing conditions. Surf. Coatings Technol. **197**(2-3), 127–136 (2005). https://doi.org/10.1016/j.surfcoat.2004.06.029
3. Paulo Davim, J., Oliveira, C., Cardoso, A.: Predicting the geometric form of clad in laser cladding by powder using multiple regression analysis (MRA). Mater Des. **29**(2), 554–557 (2008). https://doi.org/10.1016/j.matdes.2007.01.023
4. Farahmand, P., Kovacevic, R.: Parametric study and multi-criteria optimization in laser cladding by a high power direct diode laser. Lasers Manuf Mater Process. **1**(1-4), 1–20 (2014). https://doi.org/10.1007/s40516-014-0001-0
5. Lian, G., Yao, M., Zhang, Y., Chen, C.: Analysis and prediction on geometric characteristics of multi-track overlapping laser cladding. Int J Adv Manuf Technol. **97**(5-8), 2397–2407 (2018). https://doi.org/10.1007/s00170-018-2107-6
6. Alizadeh-Sh, M., Marashi, S.P.H., Ranjbarnodeh, E., Shoja-Razavi, R., Oliveira, J.P.: Prediction of solidification cracking by an empirical-statistical analysis for laser cladding of Inconel 718 powder on a non-weldable substrate. Opt Laser Technol. **128**, 106244 (2020). https://doi.org/10.1016/j.optlastec.2020.106244
7. da Silva, L.J., D'Oliveira, A.S.C.M.: NiCrSiBC coatings: effect of dilution on microstructure and high temperature tribological behavior. Wear. **350–351**, 130–140 (2016). https://doi.org/10.1016/j.wear.2016.01.015
8. Xi, W., Song, B., Zhao, Y., Yu, T., Wang, J.: Geometry and dilution rate analysis and prediction of laser cladding. Int J Adv Manuf Technol. **103**(9-12), 4695–4702 (2019). https://doi.org/10.1007/s00170-019-03932-7

9. Chai, T., Draxler, R.R.: Root mean square error (RMSE) or mean absolute error (MAE)? -arguments against avoiding RMSE in the literature. Geosci Model Dev. **7**(3), 1247–1250 (2014). https://doi.org/10.5194/gmd-7-1247-2014

10. Liu, S., Kovacevic, R.: Statistical analysis and optimization of processing parameters in high-power direct diode laser cladding. Int J Adv Manuf Technol. **74**(5-8), 867–878 (2014). https://doi.org/10.1007/s00170-014-6041-y

11. Deka, D., Das, S.P., Sahoo, N., Das, D., Jawed, M., Goyal, D., Goyal, A.: Enhanced Cellulase production from Bacillus subtilis by optimizing physical parameters for bioethanol production. ISRN Biotechnol. **2013**, 1–11 (2013). https://doi.org/10.5402/2013/965310

12. Javid, Y.: Multi-response optimization in laser cladding process of WC powder on Inconel 718. CIRP J Manuf Sci Technol. (2020). https://doi.org/10.1016/j.cirpj.2020.07.003

13. Zhao, Y., Guan, C., Chen, L., Sun, J., Yu, T.: Effect of process parameters on the cladding track geometry fabricated by laser cladding. *Optik (Stuttg)*. **223** (2020). https://doi.org/10.1016/j.ijleo.2020.165447

14. Lian, G., Yao, M., Liu, Z., Yang, S., Chen, C., Wang, H., Xiang, Y., Cong, W.: Near-net shaping control of triangular stacking in laser cladding process. Procedia Manuf. **34**, 233–238 (2019). https://doi.org/10.1016/j.promfg.2019.06.144

15. Liu, H., Hu, Z., Qin, X., Wang, Y., Zhang, J., Huang, S.: Parameter optimization and experimental study of the sprocket repairing using laser cladding. Int J Adv Manuf Technol. **91**(9-12), 3967–3975 (2017). https://doi.org/10.1007/s00170-017-0066-y

16. Scipioni, U., Wolfer, A.J., Matthews, M.J., Delplanque, J.R., Schoenung, J.M.: On the limitations of volumetric energy density as a design parameter for selective laser melting. JMADE. **113**, 331–340 (2017). https://doi.org/10.1016/j.matdes.2016.10.037

17. Salonitis, K., D'Alvise, L., Schoinochoritis, B., Chantzis, D.: Additive manufacturing and post-processing simulation: laser cladding followed by high speed machining. Int J Adv Manuf Technol. **85**(9-12), 2401–2411 (2016). https://doi.org/10.1007/s00170-015-7989-y

18. Teixeira, M.F., Veit Schmachtenberg, V.A., Tontini, G., Lana Semione, G.D., Weingaertner, W.L., Drago, V.: Laser composite surfacing of A681 steel with WC + Cr + co for improved wear resistance. J Mater Res Technol. **6**(1), 33–39 (2017). https://doi.org/10.1016/j.jmrt.2016.04.002

19. Singh, R., Kumar, D., Mishra, S.K., Tiwari, S.K.: Laser cladding of Stellite 6 on stainless steel to enhance solid particle erosion and cavitation resistance. Surf Coatings Technol. **251**, 87–97 (2014). https://doi.org/10.1016/j.surfcoat.2014.04.008

20. Xavier, M.G.C., Souza, T.M.G., Cheung, N., Garcia, A., Spinelli, J.E.: Effects of cobalt and solidification cooling rate on intermetallic phases and tensile properties of a -cu, -Zn, -Fe containing Al-Si alloy. Int J Adv Manuf Technol. **107**(1-2), 717–730 (2020). https://doi.org/10.1007/s00170-020-05077-4

21. Chen, Z., Yan, H., Zhang, P., Yu, Z., Lu, Q., Guo, J.: Microstructural evolution and wear behaviors of laser-clad Stellite 6/NbC/h-BN self-lubricating coatings. Surf. Coatings Technol. **372**, 218–228 (2019). https://doi.org/10.1016/j.surfcoat.2019.04.083

Publisher's Note Springer Nature remains neutral with regard to jurisdictional claims in published maps and institutional affiliations.

Affiliations

Jeferson Trevizan Pacheco [1,2] · Leandro João da Silva [3] · Luiz Delagnelo Barbetta [1] · Henrique Santos Ferreira [1] · Marcelo Taveira Veiga [1,2] · Renato Forni [4] · Moisés Felipe Teixeira [1,2,3,5]

[1] SENAI Innovation Institute for Manufacturing Systems and Laser Processing, Joinville, Brazil

[2] Programa de Pós-Graduação em Engenharia Mecânica – PPGEM, Universidade do Estado de Santa Catarina – UDESC, Joinville, Brazil

[3] Faculdade de Engenharia Mecânica, Universidade Federal de Uberlândia – UFU, Uberlândia, Brazil

[4] Cenpes Petrobras, Rio de Janeiro, Brazil

[5] Programa de Pós-Graduação em Ciência e Engenharia de Materiais – PGMAT, Universidade Federal de Santa Catarina – UFSC, Florianópolis, Brazil